Hierarchical glycolytic pathways control the carbohydrate utilization regulator in human gut *Bacteroides*

Seth Kabonick[a,b,c], Kamalesh Verma[a,b,c], Jennifer L. Modesto[a,b,c], Victoria H. Pearce[a,b,c], Kailyn M. Winokur[a,b,c], Eduardo A. Groisman[d], and Guy E. Townsend 2nd[a,b,c]

[a]*Penn State College of Medicine, Hershey, PA, USA*

[b]*Penn State OneHealth Microbiome Center, Pennsylvania State University, State College, PA, USA*

[c]*Center for Molecular Carcinogenesis and Toxicology, Pennsylvania State University, State College, PA, USA*

[d]*Yale University School of Medicine, New Haven, CT, USA*

*Address correspondence to Guy E. Townsend: gtownsend@pennstatehealth.psu.edu; Department of Biochemistry and Molecular Biology, Penn State College of Medicine, 700 HMC Crescent Road, Hershey, Pennsylvania, USA

Abstract

Human dietary choices control the gut microbiome. Industrialized populations consume abundant glucose and fructose, resulting in microbe-dependent intestinal disorders. Simple sugars inhibit the carbohydrate utilization regulator (Cur), a transcription factor in the prominent gut bacterial phylum, *Bacteroidetes*. Cur encodes products necessary for carbohydrate utilization, host immunomodulation, and intestinal colonization. Here, we demonstrate how simple sugars decrease Cur activity in the mammalian gut. Our findings in two *Bacteroides* species show that ATP-dependent fructose-1,6-bisphosphate (FBP) synthesis is necessary for glucose or fructose to inhibit Cur, but dispensable for growth because of an essential pyrophosphate (PPi)-dependent enzyme. Furthermore, we show that ATP-dependent FBP synthesis is required to regulate Cur in the gut but does not contribute to fitness when *cur* is absent, indicating PPi is sufficient to drive glycolysis in these bacteria. Our findings reveal how sugar-rich diets inhibit Cur, thereby disrupting *Bacteroides* fitness and diminishing products that are beneficial to the host.

Introduction

Humans can consume over 3 times the recommended amounts of glucose and fructose, monosaccharides abundant in ultra-processed foods and beverages containing high fructose corn syrup[1]. Overconsumption of these sugars supersedes the absorbative capacity of the intestine and are subsequently accessible to resident microbes[2]. High-sugar diets alter gut microbial composition and gene transcription, thereby increasing microbiota-dependent disease susceptibility[3,4]; however, the microbial processes that mediate sugar-rich, diet-dependent changes in the gut are not understood. Therefore, it is necessary to investigate the mechanisms by which refined sugar consumption reduces commensal fitness and disrupts beneficial microbiota-host interactions.

Carbon catabolite repression (CCR) is a global regulatory mechanism that prioritizes the utilization of preferred carbon sources over other available substrates[5-7]. In *Escherichia coli* (*Ec*), glucose and fructose impose CCR effects via the phosphoenolpyruvate (PEP):carbohydrate phosphotransferase system (PTS), which utilizes PEP to concomitantly import and phosphorylate target monosaccharides[8,9]. *Ec* employs the PTS to couple intracellular metabolite pools with sugar internalization and entry into central metabolism[10,11]. Ultimately, substrate phosphorylation by the PTS reduces cyclic adenosine monophosphate (cAMP), the allosteric activator of cAMP Receptor Protein (CRP), thereby preventing the transcription of CRP-activated genes which mediate the utilization of less-preferred carbon sources[8,12]. Similar to CRP in *Ec*, *Bacteroides* encodes Cur, a transcription factor that is required for growth on several carbohydrates[13-15]; however, *Bacteroides* species lack both endogenous cAMP and PTS orthologs, indicating that a distinct CCR-like mechanism controls Cur activity[16-18]. Moreover, *Bacteroides* recognizes carbohydrates and initiates transcription in the periplasm before entering central metabolism[19-21], further obscuring how sugars reduce Cur activity.

Cur regulates over 400 genes in *Bt*[15], including products necessary for glycan utilization[22], intestinal colonization[13,23], and beneficial host interactions[4]. For example, *cur* is required for fucose utilization[13,14], a constituent monosaccharide decorating host mucosal glycans that mediates a trans-kingdom signaling axis in the gut[24]. In addition, the *cur*-dependent gene, *fusA2*, encodes an alternative translation elongation factor that facilitates GTP-independent protein synthesis, a process necessary for intra-intestinal fitness[25]. Cur also regulates *BT4295* expression, which encodes an outer membrane protein that directs immunotolerogenic T-cell development to reduce host-disease susceptiblity[4]. Therefore, it is necessary to understand how simple sugars inhibit Cur activity.

Here, we report that Cur inhibition by glucose and fructose requires corresponding ATP-dependent hexokinases that facilitate their utilization. We establish that simple sugars impose CCR-like effects via a unique mechanism in the *Bacteroides*, whereby phosphorylated sugars are converted into the ubiquitous metabolite – fructose-1,6-bisphosphate (FBP) – by distinct ATP- and PPi-dependent enzymes. Strikingly, ATP-dependent FBP synthesis is required for Cur inhibition by dietary sugars and necessary for *in vivo* fitness when *cur* is present, but otherwise dispensable for cell growth. In contrast, PPi-dependent FBP synthesis is essential for growth, implying that PPi, rather than ATP, drives glycolysis in these organisms. Our findings identify unique pathways in *Bacteroides* that coordinate CCR-like effects on Cur activity in the presence of dietary sugars, thereby silencing colonization factor expression, hindering intra-intestinal fitness, and reducing products beneficial to host health.

Results

Glucose and fructose inhibit Cur activity in a dominant, dose-dependent manner.

fusA2 is the most highly upregulated *cur*-dependent gene identified to date[15]. Cur binding to the *fusA2* promoter region is necessary for transcription and fitness of *Bt* in the murine gut[15]. To kinetically examine Cur activity during growth, we generated P-*fusA2* by introducing the *fusA2* promoter into *pBolux*, a reporter plasmid containing a *Bacteroides*-optimized luciferase cassette[26]. A *wild-type Bt* strain harboring P-*fusA2* exhibited higher bioluminescence than an isogenic strain containing the promoter-less *pBolux* control plasmid in the *cur*-dependent substrates fucose and N-acetylgalactosamine (GalNAc) (Fig. 1a, b). In contrast, this strain exhibited decreasing bioluminescence during growth on the *cur*-independent monosaccharides, fructose or glucose (Fig. 1c & Extended Data Fig. 1a). When cultured in porcine mucosal O-glycans (PMOG), a mixture known to increase *cur*-dependent gene transcription[13,22], the *wild-type* strain containing P-*fusA2* produced a 45-fold increase in bioluminescence by 18 hours (Fig. 1d). Bioluminescence from P-*fusA2* requires Cur activity because a *wild-type Bt* strain harboring P-*fusA2* lacking the 22-bp Cur binding site[15] (P-*Δ22bp*) exhibited indistinguishable bioluminescence relative to strains containing *pBolux* in all conditions (Fig. 1c & Extended Data Fig. 1a, b). Similarly, a *cur*-deficient strain (*Δcur*) harboring P-*fusA2* produced bioluminescence comparable to *pBolux* when grown in identical conditions (Fig. 1c & Extended Data Fig. 1a, c). Alternatively, a *wild-type* strain harboring P-*fusA2* supplied PMOG with increasing concentrations of fructose or glucose (Fig. 1d & Extended Data Fig. 1d) elicited corresponding reductions in bioluminescence, similar to previously reported *cur*-dependent transcript levels[13]. Bioluminesence specifically reports changes in Cur activity because neither *Δcur* harboring P-*fusA2* nor the *wild-type* strain harboring P-*Δ22bp*

produced increases compared to isogenic strains harboring p*Bolux* in all examined conditions (Extended Data Fig. 1b, c, e, f). Bioluminescence did not reduce cellular growth because strains harboring P-*fusA2* or P-*Δ22bp* grew comparable to isogenic strains harboring p*Bolux* in *cur*-dependent or -independent conditions (Extended Data Fig. 1g, h, respectively). Importantly, *cur* is dispensable for reporter functionality because a strain harboring the fructose-responsive plasmid, P-*BT1763*[26], exhibited bioluminescence resembling a *wild-type Bt* strain (Extended Data Fig. 2a) when cultured in PMOG supplemented with fructose, although slightly delayed due to a growth defect (Extended Data Fig. 2b). Collectively, these data establish that glucose and fructose inhibit Cur activity in a dominant and dose-dependent manner and that P-*fusA2* faithfully reports previously observed *cur*-dependent transcript levels[13].

Cur inhibition by fructose and glucose requires ATP-dependent substrate phosphorylation.

Many other bacterial taxa alter transcription following sugar transport into the cytoplasm[27]; however, *Bacteroides* sense sugars prior to transport[26], complicating the way fructose or glucose reduce Cur activity. For example, periplasmic fructose binds the sensor protein, BT1754, which directly controls the expression of a polysaccharide utilization locus (PUL)[19] responsible for fructose utilization. Consistent with these studies, a *wild-type Bt* strain harboring P-*BT1763* exhibited increased bioluminescence during growth in PMOG containing 0.2% fructose (Extended Data Fig. 3a) and the addition of fructose increased *BT1763* transcripts 607-fold (Extended Data Fig. 3b). In contrast, a *BT1754*-deficient strain (*ΔBT1754*) produced no bioluminescence increases when harboring P-*BT1763* (Extended Data Fig. 3a) and *BT1763* transcript amounts did not significantly increase (Extended Data Fig. 3b), indicating that *BT1754* is required to transcribe genes necessary for fructose utilization, in agreement with previous findings[19,26].

The BT1754 sensor is required for fructose-dependent Cur inhibition because *ΔBT1754* harboring P-*fusA2* produced similar bioluminescence during growth in PMOG alone or in combination with 0.5% fructose (Fig. 2a). Conversely, *ΔBT1754* bioluminescence was reduced when grown in a mixture of PMOG and glucose (Fig. 2a), similar to *wild-type Bt* (Extended Data Fig. 1d). Furthermore, fructose decreased the abundance of *fusA2* and *BT4295* transcripts 181- and 747-fold, respectively, in the *wild-type* strain as previously reported[13], but had no effect in the *ΔBT1754* mutant (Fig. 2b & Extended Data Fig. 3c). In contrast, glucose addition to PMOG-grown *ΔBT1754* reduced *fusA2* and *BT4295* transcripts 809-fold and 1,784-fold, respectively, similar to the 908-fold and 2,058-fold reductions exhibited by *wild-type Bt* under identical conditions (Fig.

2b & Extended Data Fig. 3c). Therefore, BT1754 is necessary to inhibit Cur activity in response to fructose but not glucose.

The BT1754 regulon includes the putative fructokinase-encoding gene, *BT1757*. Accordingly, *BT1757* transcripts increased 33-fold in a BT754-dependent manner following the introduction of fructose (Fig. 2c), BT1757 protein possessed *in vitro* fructokinase activity (Fig. 2d), and a *BT1757*-deficient strain (*ΔBT1757*) was unable to grow on fructose (Fig. 2e). In contrast, *ΔBT1757* did not exhibit a growth defect in glucose (Extended Data Fig. 3d) or PMOG (Extended Data Fig. 3e), indicating that this enzyme is likely the sole *Bt* fructokinase. Fructose phosphorylation is required for entry into central metabolism, but not necessary for BT1754-directed PUL transcription, because *ΔBT1757* harboring P-*BT1763* exhibited increased bioluminescence (Extended Data Fig. 3a) and *BT1763* transcript amounts increased 210-fold in *ΔBT1757* following the introduction of fructose (Extended Data Fig. 3b). Conversely, *BT1763* transcript amounts did not increase in *ΔBT1754* (Extended Data Fig. 3b). BT1757 is necessary for fructose-dependent Cur inhibition because *ΔBT1757* harboring P-*fusA2* produced similar bioluminescence during growth in PMOG or a combination of PMOG and fructose but exhibited reduced bioluminescence during growth in PMOG and glucose mixture (Fig. 2f), similar to *wild-type Bt* (Extended Data Fig. 1d) and *ΔBT1754* (Fig. 2a). Thus, fructose specifically decreases Cur activity via this compartmentalized signaling machinery by increasing fructokinase transcription, suggesting that sugar phosphorylation is necessary to reduce Cur activity.

We predicted that glucose phosphorylation mediates Cur inhibition by a distinct mechanism, likely involving a hexokinase, because glucose addition reduced Cur activity independent of fructokinase (Fig. 2b and Fig. 2f). We determined that the putative hexokinase, BT2493, exhibits glucokinase activity *in vitro* (Extended Data Fig. 4a) and a *BT2493*-deficient strain (*ΔBT2493*) was unable to grow on glucose, but grew similarly to *wild-type Bt* in media containing fructose or PMOG (Extended Data Fig. 4b). Accordingly, *ΔBT2493* harboring P-*fusA2* exhibited similar bioluminescence during growth in media containing PMOG or equal amounts of PMOG and glucose (Fig. 2g). Neither *fusA2* nor *BT4295* transcripts decreased following the addition of 0.2% glucose to *ΔBT2493* growing on PMOG (Fig. 2h); however, fructose-dependent silencing resembled *wild-type Bt* (Fig. 2b), indicating that *BT2493* is necessary for glucose, but not fructose, to inhibit Cur activity. Therefore, glucose and fructose require distinct ATP-dependent hexokinases for their utilization and inhibition of Cur activity.

_Bt_ possesses both ATP- and PPi-dependent phosphofructokinases.

In the Ebden-Meyerhoff-Parnas (EMP) pathway, phosphoglucoisomerase (Pgi) converts glucose-6-phosphate (G6P) into fructose-6-phosphate (F6P), which is subsequently phosphorylated into FBP (Fig. 3a). Because FBP synthesis is the primary regulatory step in glycolysis and *wild-type Bt* cells exhibit reduce FBP amounts[28] with corresponding increases in Cur activity during carbon limitation[13,15], we hypothesized that glucose and fructose reduce Cur activity via this glycolytic step. To test this, we first examined the biochemical activities of 3 putative *Bt* phosphofructokinase (Pfk) enzymes: BT1102, BT2062, and BT3356, whose amino acid sequences share greater than 45% identity with *Ec pfkA* (Extended Data Fig. 5a). We determined that BT2062 and BT1102, but not BT3356, are *bona fide* ATP-dependent Pfks because expression of each in a *pfk*-deficient *Ec* strain[29] restored growth on glucose (Extended Data Fig. 5b) when expressed in an inducer-dependent manner (Extended Data Fig. 5c). Moreover, purified recombinant BT2062 and BT1102 proteins exhibited Pfk activity *in vitro*, whereas BT3356 did not (Fig. 3b). Therefore, like *Ec, Bt* encodes two Pfk enzymes that convert F6P into FBP using ATP (Fig. 3a).

Bacteroides species also encode a putative fructose-6-phosphate 1-phosphotransferase (Pfp), BT0307, which synthesizes FBP independently of ATP by utilizing pyrophosphate (PPi) as a phosphoryl donor. BT0307 exhibited PPi-dependent FBP synthesis *in vitro*, whereas PfkA and PfkB did not (Fig. 3c). *Bt* expresses *pfkA*, *pfkB*, and *pfp* simultaneously during growth in PMOG and the addition of glucose or fructose decreased *pfkB* and increased *pfp* 2-fold, respectively, but had no effect on *pfkA* transcript amounts (Extended Data Fig. 5d). These results suggest that both ATP- and PPi-dependent FBP synthesis occur simultaneously in the cell; however, FBP synthesis is likely governed by intracellular PPi amounts, because PfkA activity was potently inhibited by PPi *in vitro* (Fig. 3d). Furthermore, PMOG grown *wild-type Bt* exhibited 2.5-fold higher PPi amounts that in fructose-containing media (Fig. 3e), suggesting that fructose utilization permits ATP-dependent FBP synthesis by reducing PPi levels below inhibitory concentrations. Thus, in contrast to other enteric bacteria, *Bt* employs divergent FBP biosynthetic pathways.

ATP-dependent FBP synthesis controls Cur activity.

To investigate the role of FBP synthesis in Cur inhibition, we constructed mutants with deletions in *pfkA* (*ΔpfkA*), *pfkB* (*ΔpfkB*), or both *pfkA* and *pfkB genes* (*ΔpfkAB*). *ΔpfkB* grew like *wild-type Bt,* whereas *ΔpfkA* had slightly increased growth rates and maxima in fructose (Fig. 4a). Unexpectedly, *ΔpfkAB* grew similarly to or better than *wild-type Bt* on fructose (Fig. 4a), glucose, or PMOG (Extended Data Fig. 6a, b), implying that ATP-dependent FBP synthesis is dispensable for *in vitro* growth. Cell extracts prepared from *ΔpfkA* or *ΔpfkAB* exhibited no Pfk activity, indicating

that ATP-dependent FBP synthesis was entirely absent in these strains (Fig. 4b). In contrast, extracts prepared from *wild-type* and *ΔpfkA* produced indistinguishable PPi-dependent FBP synthesis *in vitro* at rates 11.2- and 38.5-fold greater than ATP-dependent reactions, respectively (Fig. 4b). Conversely, we were unable to generate a strain lacking the *BT0307* open-reading frame, suggesting *pfp* is necessary for growth (Extended Data Fig. 6c), which agrees with transposon-based examinations of essential genes in *Bt*[30,31]. Therefore, PPi-dependent FBP synthesis provides sufficient metabolic flux, thereby rendering ATP-dependent FBP synthesis dispensable for growth.

To determine how Pfk enzymes support glycolysis, we measured steady-state metabolite abundances in *wild-type*, *ΔpfkA, ΔpfkB,* and *ΔpfkAB Bt* strains. Accordingly, *ΔpfkA* and *ΔpfkAB* exhibited respective 2.9-fold and 2.7-fold lower steady-state FBP amounts in bacteria grown on glucose and fructose, respectively, whereas *ΔpfkB* showed no significant changes in either condition (Fig. 4c & Extended Data Fig. 7a) indicating that PfkA is the dominant ATP-dependent FBP biosynthetic enzyme in *Bt*. Downstream glycolytic metabolites, such as dihydroxyacetone phosphate (DHAP), also exhibited corresponding reductions in *ΔpfkA* but not *ΔpfkB* grown in either glucose or fructose (Fig. 4c & Extended Data Fig. 7b). Conversely, PEP and pyruvate amounts were similar across all strains and conditions (Fig. 4c & Extended Data Fig. 7c, d), suggesting these metabolites are maintained by processes independent of *pfkA* and *pfkB*. Additionally, *ΔpfkAB* resembled *ΔpfkA* across all metabolites and conditions (Fig. 4c & Extended Data Fig. 7a-d). Finally, ATP-dependent FBP synthesis is necessary for maintaining steady-state NTPs and reducing equivalents because ATP and NADH amounts were also reduced in *ΔpfkA* and *ΔpfkAB* (Fig. 4c).

To determine if ATP-dependent FBP synthesis contributes to Cur inhibition, we measured bioluminescence in isogenic *wild-type*, *ΔpfkA*, *ΔpfkB*, and *ΔpfkAB* harboring P-*fusA2*. Strikingly, *ΔpfkA* exhibited a 9.2-fold increase in bioluminescence by 12 hours during growth in equal amounts of fructose and PMOG (Fig. 4d) and increased 10.5-fold by the same time point in glucose and PMOG (Extended Data Fig. 8a). Bioluminescence increased further in *ΔpfkAB* over *ΔpfkA,* however, *ΔpfkB* exhibited bioluminescence comparable to *wild-type Bt* harboring an identical reporter plasmid during growth on either mixture (Fig. 4d & Extended Data Fig. 8a). Similarly, *ΔpfkA* and *ΔpfkAB* produced greater bioluminescence during growth on glucose, fructose, and PMOG as sole carbon sources (Extended Data Fig. 8b-d), suggesting that disabling ATP-dependent FBP synthesis increases Cur activity.

Consistent with observed bioluminescence increases, *ΔpfkA*, but not *ΔpfkB*, is required for Cur inhibition by glucose and fructose because *fusA2*, *BT4295*, and *fucI* transcript amounts increased 9.1-, 37.2-, and 3.7-fold respectively when grown on fructose as the sole carbon source, whereas *ΔpfkB* exhibited transcript amounts indistinguishable from *wild-type* (Fig. 4e). Similarly, *ΔpfkA* exhibited respective 2.7-, 6-, and 1.7-fold increased *fusA2* (Fig. 4f), *BT4295* (Extended Data Fig. 8e), and *fucI* (Extended Data Fig. 8f) transcript amounts during growth in glucose that were abolished when the *pfkA* gene was supplied *in trans* (Fig. 4f, Extended Data Fig. 8e-f). The amounts of all three transcripts were indistinguishable between *Δcur* and *ΔpfkA Δcur*; but increased in *ΔpfkA Δcur* complemented *in trans* with *cur* but not *pfkA* (Fig. 4f, Extended Data Fig. 8e-f).

To explore the possibility of glycolytic intermediates directly impacting Cur's ability to bind its regulated promoters, we performed electromobility shift assays with purified Cur protein and the *wild-type fusA2* promoter or a *Δ22*bp control probe. Accordingly, increasing concentrations of Cur protein shifted the *wild-type fusA2*, but not the *Δ22*bp probe (Extended Data Fig. 9a-b). Cur activity is not directly regulated by glycolytic intermediates that were differentially abundant in *ΔpfkA* because *fusA2* probe shifting was unaltered when F6P, FBP, DHAP, and PEP were included in the assay (Extended Data Fig. 9c). Thus, ATP-dependent FBP synthesis appears to control Cur activity indirectly.

ATP-dependent FBP synthesis regulates Cur *in vivo*.

We hypothesized that PfkA may play a role in intra-intestinal *Bt* fitness because *ΔpfkA* exhibited increased *cur*-dependent products in the presence of simple sugars. Therefore, we inoculated germ-free mice with equal amounts of *wild-type* and *ΔpfkA* and followed their abundance over time. *pfkA* confers a fitness advantage *in vivo* because the relative abundance of *ΔpfkA* decreased 135-fold after 2 weeks (Fig. 5a). This suggests that the demands of intra-intestinal life require ATP-dependent FBP production even though this process reduces growth *in vitro* (Fig. 4a). We also examined the relative abundances of *Δcur* and *ΔpfkA Δcur* following co-introduction into germ-free mice. Strikingly, both strains were present at nearly indistinguishable abundances across two weeks, suggesting that sole purpose of *pfkA* is to regulate Cur in the mammalian intestine (Fig. 5b).

Because *pfkA* is required for reducing *cur*-dependent products (Fig. 4f and Extended Data Fig. 8e-f), we reasoned that a high sugar diet would ameliorate the *ΔpfkA* fitness defect by inhibiting Cur activity in *wild-type Bt*. Accordingly, *ΔpfkA* abundance was reduced only 1.4-fold

compared to *wild-type Bt* after 2 weeks in mice provided a sugar-rich chow (Fig. 5a). This indicates that dietary sugar inhibits Cur activity *in vivo* and reduces the *wild-type* strain's advantage over *ΔpfkA*. Finally, sugar-dependent effects on Cur activity are responsible for decreased *Bt* fitness because the abundances of *Δcur* and *ΔpfkA Δcur* were indistinguishable following introduction into germ-free mice fed a simple sugar-rich diet (Fig. 5b). Taken together, our data demonstrate that ATP-dependent FBP synthesis benefits *Bt* by regulating Cur activity in the mammalian gut and that *pfkA* activity is required for dietary sugars to inhibit Cur.

PfkA regulates Cur activity across human intestinal *Bacteroides* species.

Along with *Bt*, human *Bacteroides* isolates *B. fragilis (Bf)*, *B. ovatus*, and *Phocaeicola vulgatus* employ Cur to regulate their corresponding *fusA2* orthologs and *Bf* exhibits identical transcript silencing in response to glucose or fructose addition during growth in PMOG[13]. Each species also encodes *pfkA* orthologs (*BF9343_3444*, *BACOVA_00639*, and *BVU_1935*, respectively) and *pfp* orthologs (*BF9343_2852*, *BACOVA_01648*, and *BVU_2286*, respectively) suggesting that ATP-dependent FBP synthesis could govern Cur activity across *Bacteroides* species. We introduced P-*Bf-fusA2 (*p*Bolux* containing the 300 bp region preceding *BF9343_3536)* into *wild-type Bf* and isogenic strains lacking the *pfkA*-ortholog, *BF9343_3444* (*ΔpfkA*) or *cur*-ortholog, *BF9343_0915* (*Δcur*). A *wild-type* strain harboring P-*Bf-fusA2* exhibited a 12.3-fold increase in bioluminescence compared to a strain harboring a promoter-less p*Bolux* during growth in PMOG (Extended Data Fig. 10a), displaying trends similar to *wild-type Bt* harboring P-*fusA2* (Fig. 1d). In contrast, an identical strain exhibited 2.3-fold increased bioluminescence compared to the promoter-less control strain during growth in either glucose (Extended Data Fig. 10b) or fructose (Extended Data Fig. 10c) as a sole carbon source. The addition of glucose (Fig. 6a) or fructose (Fig. 6b) to PMOG reduced bioluminescence from *wild-type* harboring P-*Bf-fusA2* whereas *ΔpfkA* displayed increased bioluminescence under all conditions (Fig. 6a-b & Extended Data Fig. 10a-c). As expected, cell extracts from *ΔpfkA* exhibited no ATP-dependent FBP synthesis *in vitro* compared to *wild-type* (Fig. 6c), collectively indicating that this process inhibits Cur activity in *Bf*. Consistent with this notion, bioluminescence from a *Bf* strain lacking both *pfkA* and *cur* (*ΔpfkA Δcur*) was indistinguishable from one lacking only *cur* (*Δcur)*, which were lower than isogenic strains harboring the promoter-less p*Bolux* plasmid (Fig. 6a-b, and Extended Data Fig. 10a-c). Therefore, Cur inhibition by ATP-dependent FBP production during growth in dietary sugars is conserved among human *Bacteroides* species.

Discussion

Our work reveals a pathway in human intestinal *Bacteroides* species required for glucose and fructose to inhibit Cur. We determined that phosphorylation of either monosaccharide requires ATP-dependent sugar kinases necessary for growth, a strategy distinct from traditional PTS that utilize PEP to phosphorylate sugars upon transport (Fig. 2). Furthermore, we show that *Bt* possesses both ATP- and PPi-dependent enzymes, Pfk and Pfp respectively, which form a hierarchical paradigm to regulate FBP synthesis (Fig. 3) and control Cur activity in response to nutrient availability. We demonstrate that eliminating Pfk alleviates sugar-dependent Cur inhibition without reducing growth (Fig. 4); however, *pfkA* is necessary to control Cur during intestinal colonization (Fig. 5). Furthermore, ATP-dependent FBP synthesis inhibits Cur *in vivo* because the competitive defect exhibited by *⊿pfkA* (Fig. 5b) is abolished when simple sugars are abundant in the host diet. Finally, we established that these processes are conserved in *B. fragilis* and are likely shared among the *Bacteroides* (Fig. 6).

Bacteroides abundance is markedly decreased following murine consumption of dietary sugar[32] and Cur controls the expression of genes necessary to ferment dietary carbohydrates into host-absorbable nutrients[13]. Our findings explain how glucose and fructose consumption hinder *Bacteroides* intestinal fitness by exerting CCR-like effects on Cur activity via two hierarchical FBP biosynthetic pathways. Remarkably, PPi-dependent FBP synthesis occurs at a nearly 12-fold higher rate than ATP-dependent reactions; yet eliminating ATP-dependent synthesis when glucose or fructose is readily available reduced steady-state FBP levels by more than 50% (Extended Data Fig. 7a, b). To explain this phenomenon, we propose that the utilization of these simple sugars reduces PPi levels below an inhibitory threshold, thereby simultaneously diminishing the activity of Pfp and removing the inhibitory effect of PPi on PfkA. Furthermore, the essentiality of *pfp*[33] (Extended Data Fig. 6c) and lack of native pyrophosphorylase[34] imply that *Bacteroides* have evolved to rely on PPi, rather than ATP, as a significant glycolytic energy source to conserve ATP pools. A similar energy-conservation strategy is employed in *Bt* via the *cur*-dependent gene, *fusA2*, which encodes a product that preserves NTP pools by facilitating GTP-independent protein synthesis[25]. A deeper examination into the role of PPi-dependent reactions across gut commensals is necessary to understand how bacteria balance NTP and PPi pools to govern intestinal colonization.

FBP is a ubiquitous metabolite that serves as both a glycolytic intermediate and metabolic regulator of other crucial energy pathways[35]. Because endogenous FBP levels are inversely related to Cur activity[28], but do not directly alter Cur activity (Extended Data Fig. 8c), we hypothesize that FBP regulates other important energy pathways in *Bacteroides.* For example,

328 FBP is required to stimulate glycogen production in the *Bacteroidetes* family member, *Prevotella*
329 *bryantii*[36]. Intriguingly, *Bt* genes encoding putative glycogen metabolic enzymes are important
330 fitness determinants in the murine intestine[30,31] and are necessary for fitness in *cur*-dependent,
331 but not -independent, substrates[33]. In light of this, we propose that host consumption of abundant
332 glucose and fructose reconfigures central metabolism by stimulating ATP-dependent FBP
333 synthesis and glycogenesis, in-turn reducing an unknown Cur activator, and ultimately disrupting
334 products necessary for *Bacteroides* fitness and beneficial host interactions.

Methods

Bacterial strains and growth conditions

All bacteria were cultured as described previously[13] except for *ΔBT2493* strains, which were cultured on rich and minimal media preparations where glucose was replaced with identical concentrations of fructose.

Engineering chromosomal deletions

Indicated *Bt* genomic deletions were generated using pEXCHANGE-*tdk* plasmids harboring flanking sequences, amplified using the primers listed in Supplementary Table 2, as previously described[37]. Indicated *Bf* genomic deletions were generated using pLGB13 plasmids harboring flanking sequences, amplified using the primers listed in Supplementary Table 2, as previously described[13,38].

Bacterial growth assays

Bacterial growth was measured as previously described[13].

Transcription reporter assays

Bioluminescence from each strain was measured in a Tecan Infinite M Plex for 18 hours following 1:200 dilution of stationary phase culture in rich media into freshly prepared minimal media containing the indicated carbon sources. Each measurement was normalized to isogenic strains harboring the promoter-less p*Bolux* plasmid as previously described[26].

qPCR

Transcripts were measured as previously described using a QuantStudio5 (ThermoFisher) and PowerUp SYBR Green Master Mix (ThermoFisher) with amplicon specific primers listed in Supplementary Table 1.

E. coli complementation

Plasmids harboring putative *pfk* genes were introduced into the *pfkAB*-deficient *E. coli* strain as previously described[29]. The resulting strains were cultured in M9 minimal media containing glucose as the sole carbon source supplemented with 100 μM IPTG.

Protein expression and purification

Protein overexpression and purification was carried out as previously described, with the following modifications: inserts encoding each enzyme were amplified from *B. thetaiotaomicron* VPI-5482 genomic DNA and cloned into pT7-7-N6H4A linearized with NotI-HF (NEB) and HindIII-HF (NEB) using NEBuilder Hi-Fi Master Mix (NEB). N-terminally hexa-histidine-tagged proteins were eluted from Ni^{2+}-NTA resin (Thermo) with 250 mM imidazole, followed by buffer exchange using appropriate MWCO centrifugal concentrators (MilliporeSigma).

Enzyme assays

Crude lysates and recombinant enzymes were tested by coupling glycolytic reactions with NADH oxidation using an excess of the axillary glycolytic enzymes aldolase (ALD), triose phosphate isomerase (TPI), and glyceraldehyde 3-phosphate dehydrogenase (GDH) (MilliporeSigma). All reactions were performed with 5 µg of enzyme, or 50 µL of lysate, in 100 µL buffer containing of 50 mM Tris (pH = 7.4), 3 mM $MgCl_2$, and 10 mM NH_4Cl. The degradation of NADH was kinetically measured using absorbance at 340 nm with a Tecan Spark. Changes in absorbance across a five-minute linear slope was converted to moles of NADH consumed using a standard curve and normalized by the amount of enzyme to yield the enzymatic rate (nmol/min/µg protein). Enzyme activities were analyzed using non-linear regression and fit to Michaelis-Menten models using GraphPad Prism. PPi inhibition assays were performed in an identical manner with 5 µg of enzyme and 20 mM substrate and fit to a dose-response model.

Quantification of pyrophosphate

Wild-type Bt was subbed 1:50 from rich media to minimal media containing the indicated carbon source and grown to mid-logarithmic phase (OD~0.45 - 0.65). Cells pellets were resuspended in 1 mL buffer containing of 50 mM Tris (pH = 7.4), 3 mM $MgCl_2$, and 10 mM NH_4Cl and immediately boiled. PPi was quantified in resulting extracts using a high sensitivity detection kit (Sigma Aldrich) according to the manufacturer's directions.

Electromobility shift assays

DNA fragments containing the *fusA2* promoter region were amplified by PCR using Q5 High Fidelity Master Mix and isolated from an agarose gel using a QIAquick gel extraction kit (QIAGEN). Equal amounts of probe and 2 mg/mL poly-dI/dC (MilliporeSigma) were combined with purified Cur protein in binding buffer (20 mM HEPES (pH = 8.0) 10 mM KCl, 2 mM $MgCl_2$, 0.1 mM EDTA, 0.1 mM dithiothreitol (DTT), and 10% glycerol) to a final volume of 20 µL. Reactions were incubated for 20 minutes at room temperature with 4 µL of 6x Native loading buffer, followed by a

second, 12-hour incubation at room temperature. Samples were loaded onto a 4-20% TBE gel (Life Technologies), preconditioned in 0.38% TBE, and electrophoresed for 3 hours at 100V. Gels were stained using SYBR green (Invitrogen) per the manufacturer's directions and imaged using an AI680 (GE).

Metabolomics

Bt strains were cultured in minimal media containing 5 mg/mL glucose to mid-logarithmic phase (OD~0.45 - 0.65) where 0.5 ODs were collected by centrifugation for 30 seconds, quickly decanted, and immediately flash frozen in a mixture of ethanol and dry ice. Metabolite abundances were measured using Targeted Quantification Analysis by LC-MRM/MS at Creative Proteomics.

In vivo competitive fitness of B. thetaiotaomicron strains

All animal experiments were performed in accordance with protocols approved by Penn State Institutional Animal Care and Use Committee. Germ-free C57/BL6 mice were maintained in flexible plastic gnotobiotic isolators with a 12-hour light/dark cycle and provided a standard, autoclaved mouse chow (LabDiet, 5021) or high-sugar chow (Bioserv, S4944) *ad libitum*. Mice were gavaged with 10^8 CFU of each indicated strains suspended in 200 µL of phosphate-buffered saline. Input (day 0) abundance of each strain was determined by CFU plating. Fecal pellets were collected at the desired times and genomic DNA was extracted as described previously[15]. The abundance of each strain was measured by qPCR, using barcode-specific primers (Supplemental Table 2) as described previously[13].

Acknowledgements

We thank Jordan Bisanz, Donalee McElrath, Michelle Irish, Jacob Perryman, and Alexandra Sprinkle for assistance with germ-free mouse experiments. Additionally, we thank Andrew Goodman, Whitman Schofield, Andrew Patterson, and Imhoi Koo for insights about metabolite measurements. This work was supported, in part, by National Institutes of Health Grants DK132711 and GM147178 to G.E.T. and GM123798 to E.A.G.

References

1 Lee, S. H. *et al.* High Added Sugars Intake among US Adults: Characteristics, Eating Occasions, and Top Sources, 2015-2018. *Nutrients* **15**, doi:10.3390/nu15020265 (2023).

2 Jang, C. *et al.* The Small Intestine Converts Dietary Fructose into Glucose and Organic Acids. *Cell Metab* **27**, 351-361 e353, doi:10.1016/j.cmet.2017.12.016 (2018).

3 Khan, S. *et al.* Dietary simple sugars alter microbial ecology in the gut and promote colitis in mice. *Sci Transl Med* **12**, doi:10.1126/scitranslmed.aay6218 (2020).

4 Wegorzewska, M. M. *et al.* Diet modulates colonic T cell responses by regulating the expression of a Bacteroides thetaiotaomicron antigen. *Sci Immunol* **4**, doi:10.1126/sciimmunol.aau9079 (2019).

5 Magasanik, B. Catabolite repression. *Cold Spring Harb Symp Quant Biol* **26**, 249-256, doi:10.1101/sqb.1961.026.01.031 (1961).

6 Loomis, W. F., Jr. & Magasanik, B. The catabolite repression gene of the lac operon in Escherichia coli. *J Mol Biol* **23**, 487-494, doi:10.1016/s0022-2836(67)80120-7 (1967).

7 Bruckner, R. & Titgemeyer, F. Carbon catabolite repression in bacteria: choice of the carbon source and autoregulatory limitation of sugar utilization. *FEMS Microbiol Lett* **209**, 141-148, doi:10.1111/j.1574-6968.2002.tb11123.x (2002).

8 Saier, M. H., Jr., Feucht, B. U. & Hofstadter, L. J. Regulation of carbohydrate uptake and adenylate cyclase activity mediated by the enzymes II of the phosphoenolpyruvate: sugar phosphotransferase system in Escherichia coli. *J Biol Chem* **251**, 883-892 (1976).

9 Simoni, R. D., Roseman, S. & Saier, M. H., Jr. Sugar transport. Properties of mutant bacteria defective in proteins of the phosphoenolpyruvate: sugar phosphotransferase system. *J Biol Chem* **251**, 6584-6597 (1976).

10 Deutscher, J., Francke, C. & Postma, P. W. How phosphotransferase system-related protein phosphorylation regulates carbohydrate metabolism in bacteria. *Microbiol Mol Biol Rev* **70**, 939-1031, doi:10.1128/MMBR.00024-06 (2006).

11 Somavanshi, R., Ghosh, B. & Sourjik, V. Sugar Influx Sensing by the Phosphotransferase System of Escherichia coli. *PLoS Biol* **14**, e2000074, doi:10.1371/journal.pbio.2000074 (2016).

12 Stulke, J. & Hillen, W. Carbon catabolite repression in bacteria. *Curr Opin Microbiol* **2**, 195-201, doi:10.1016/S1369-5274(99)80034-4 (1999).

13 Pearce, V. H., Groisman, E. A. & Townsend, G. E., 2nd. Dietary sugars silence the master regulator of carbohydrate utilization in human gut Bacteroides species. *Gut Microbes* **15**, 2221484, doi:10.1080/19490976.2023.2221484 (2023).

14 Schwalm, N. D., 3rd, Townsend, G. E., 2nd & Groisman, E. A. Multiple Signals Govern Utilization of a Polysaccharide in the Gut Bacterium Bacteroides thetaiotaomicron. *mBio* **7**, doi:10.1128/mBio.01342-16 (2016).

15 Townsend, G. E., 2nd *et al.* A Master Regulator of Bacteroides thetaiotaomicron Gut Colonization Controls Carbohydrate Utilization and an Alternative Protein Synthesis Factor. *mBio* **11**, doi:10.1128/mBio.03221-19 (2020).

16 Barabote, R. D. & Saier, M. H., Jr. Comparative genomic analyses of the bacterial phosphotransferase system. *Microbiol Mol Biol Rev* **69**, 608-634, doi:10.1128/mmbr.69.4.608-634.2005 (2005).

17 Siegel, L. S., Hylemon, P. B. & Phibbs, P. V., Jr. Cyclic adenosine 3',5'-monophosphate levels and activities of adenylate cyclase and cyclic adenosine 3',5'-monophosphate phosphodiesterase in Pseudomonas and Bacteroides. *J Bacteriol* **129**, 87-96, doi:10.1128/jb.129.1.87-96.1977 (1977).

18 Hylemon, P. B. & Phibbs, P. V., Jr. Evidence against the presence of cyclic AMP and related enzymes in selected strains of Bacteroides fragilis. *Biochem Biophys Res Commun* **60**, 88-95, doi:10.1016/0006-291x(74)90176-4 (1974).

19 Sonnenburg, E. D. *et al.* Specificity of polysaccharide use in intestinal bacteroides species determines diet-induced microbiota alterations. *Cell* **141**, 1241-1252, doi:10.1016/j.cell.2010.05.005 (2010).

20 Raghavan, V., Lowe, E. C., Townsend, G. E., 2nd, Bolam, D. N. & Groisman, E. A. Tuning transcription of nutrient utilization genes to catabolic rate promotes growth in a gut bacterium. *Mol Microbiol* **93**, 1010-1025, doi:10.1111/mmi.12714 (2014).

21 Lowe, E. C., Basle, A., Czjzek, M., Firbank, S. J. & Bolam, D. N. A scissor blade-like closing mechanism implicated in transmembrane signaling in a Bacteroides hybrid two-component system. *Proc Natl Acad Sci U S A* **109**, 7298-7303, doi:10.1073/pnas.1200479109 (2012).

22 Ryan, D. *et al.* An expanded transcriptome atlas for Bacteroides thetaiotaomicron reveals a small RNA that modulates tetracycline sensitivity. *Nat Microbiol* **9**, 1130-1144, doi:10.1038/s41564-024-01642-9 (2024).

23 Townsend, G. E., 2nd *et al.* Dietary sugar silences a colonization factor in a mammalian gut symbiont. *Proc Natl Acad Sci U S A* **116**, 233-238, doi:10.1073/pnas.1813780115 (2019).

24 Bry, L., Falk, P. G., Midtvedt, T. & Gordon, J. I. A model of host-microbial interactions in an open mammalian ecosystem. *Science* **273**, 1380-1383, doi:10.1126/science.273.5280.1380 (1996).

25 Han, W. *et al.* Gut colonization by Bacteroides requires translation by an EF-G paralog lacking GTPase activity. *EMBO J*, e112372, doi:10.15252/embj.2022112372 (2022).

26 Modesto, J. L., Pearce, V. H. & Townsend, G. E., 2nd. Harnessing gut microbes for glycan detection and quantification. *Nat Commun* **14**, 275, doi:10.1038/s41467-022-35626-2 (2023).

27 Carreon-Rodriguez, O. E., Gosset, G., Escalante, A. & Bolivar, F. Glucose Transport in Escherichia coli: From Basics to Transport Engineering. *Microorganisms* **11**, doi:10.3390/microorganisms11061588 (2023).

28 Schofield, W. B., Zimmermann-Kogadeeva, M., Zimmermann, M., Barry, N. A. & Goodman, A. L. The Stringent Response Determines the Ability of a Commensal Bacterium to Survive Starvation and to Persist in the Gut. *Cell Host Microbe* **24**, 120-132 e126, doi:10.1016/j.chom.2018.06.002 (2018).

29 Lovingshimer, M. R., Siegele, D. & Reinhart, G. D. Construction of an inducible, pfkA and pfkB deficient strain of Escherichia coli for the expression and purification of phosphofructokinase from bacterial sources. *Protein Expr Purif* **46**, 475-482, doi:10.1016/j.pep.2005.09.015 (2006).

30 Goodman, A. L. *et al.* Identifying genetic determinants needed to establish a human gut symbiont in its habitat. *Cell Host Microbe* **6**, 279-289, doi:10.1016/j.chom.2009.08.003 (2009).

31 Liu, H. *et al.* Functional genetics of human gut commensal Bacteroides thetaiotaomicron reveals metabolic requirements for growth across environments. *Cell Rep* **34**, 108789, doi:10.1016/j.celrep.2021.108789 (2021).

32 Turnbaugh, P. J. *et al.* The effect of diet on the human gut microbiome: a metagenomic analysis in humanized gnotobiotic mice. *Sci Transl Med* **1**, 6ra14, doi:10.1126/scitranslmed.3000322 (2009).

33 Price, M. N. *et al.* Mutant phenotypes for thousands of bacterial genes of unknown function. *Nature* **557**, 503-509, doi:10.1038/s41586-018-0124-0 (2018).

34 Kuil, T., Nurminen, C. M. K. & van Maris, A. J. A. Pyrophosphate as allosteric regulator of ATP-phosphofructokinase in Clostridium thermocellum and other bacteria with ATP- and PP(i)-phosphofructokinases. *Arch Biochem Biophys* **743**, 109676, doi:10.1016/j.abb.2023.109676 (2023).

35 Wang, C. Y. *et al.* Metabolome and proteome analyses reveal transcriptional misregulation in glycolysis of engineered E. coli. *Nat Commun* **12**, 4929, doi:10.1038/s41467-021-25142-0 (2021).

36 Lou, J., Dawson, K. A. & Strobel, H. J. Glycogen biosynthesis via UDP-glucose in the ruminal bacterium Prevotella bryantii B1(4). *Appl Environ Microbiol* **63**, 4355-4359, doi:10.1128/aem.63.11.4355-4359.1997 (1997).

37 Koropatkin, N. M., Martens, E. C., Gordon, J. I. & Smith, T. J. Starch catabolism by a prominent human gut symbiont is directed by the recognition of amylose helices. *Structure* **16**, 1105-1115, doi:10.1016/j.str.2008.03.017 (2008).

38 Garcia-Bayona, L. & Comstock, L. E. Streamlined Genetic Manipulation of Diverse Bacteroides and Parabacteroides Isolates from the Human Gut Microbiota. *mBio* **10**, doi:10.1128/mBio.01762-19 (2019).

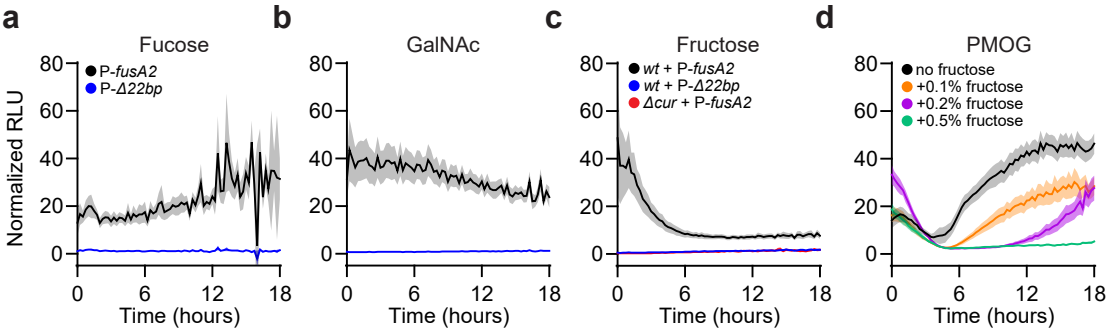

Fig. 1. A bioluminescent transcriptional reporter of Cur activity. a,b, Bioluminescence from a *wild-type Bt* strain harboring P-*fusA2* (black) or P-Δ*22bp* (blue) were cultured in media containing **(a)** fucose or **(b)** GalNAc as the sole carbon source normalized to measurements collected from isogenic strains harboring a promoter-less p*Bolux* plasmid. **c,** Normalized bioluminescence from a *wild-type* strain harboring P-*fusA2* (black) or P-Δ*22bp* (blue) and a Δ*cur Bt* strain harboring P-*fusA2* (red) cultured in fructose as a sole carbon source. **d,** Normalized bioluminescence from a *wild-type Bt* strain harboring P-*fusA2* cultured in PMOG alone (black) or in combination with 0.1% (orange), 0.2% (purple), or 0.5% (green) fructose. For panels **a-d,** n=8, error is SEM in color matched shading.

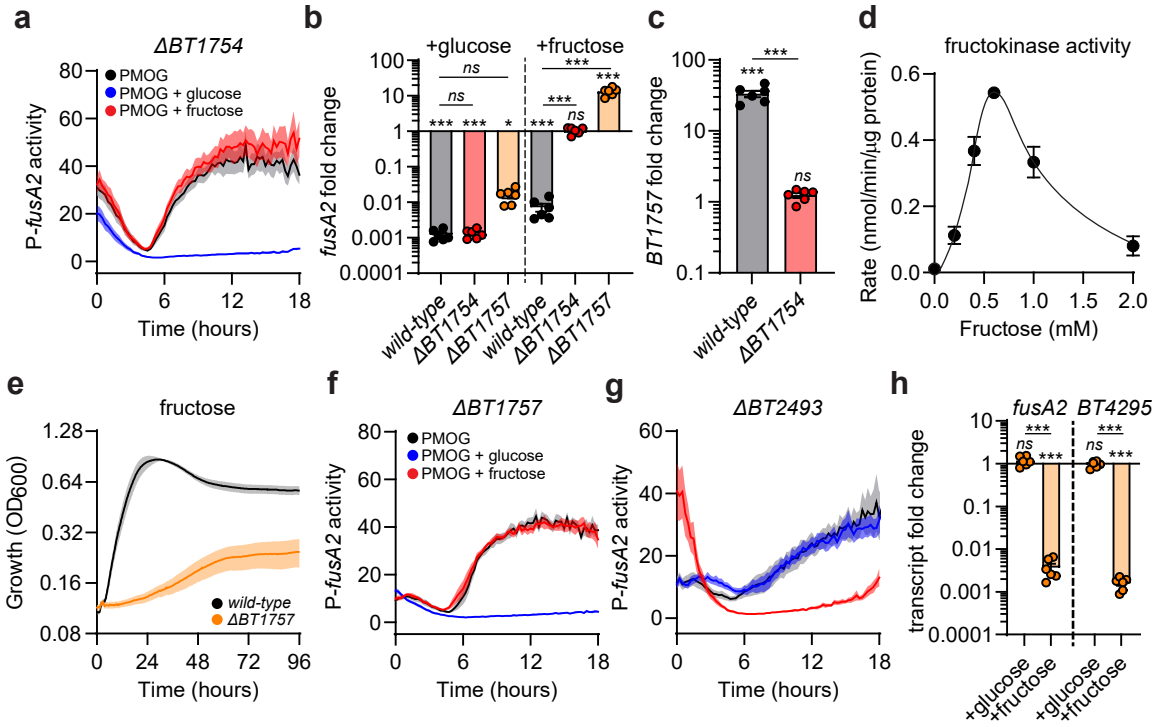

Fig. 2. Fructose and glucose require phosphorylation for Cur inhibition. a, Normalized bioluminescence from *Δ BT1754* harboring P-*fusA2* cultured in media containing PMOG (black), PMOG and fructose (red), or PMOG and glucose (blue). **b,** Fold change of *fusA2* transcript amounts from *wild-type* (black), *ΔBT1754* (red), and *ΔBT1757* (orange) cultured in media containing PMOG as the sole carbon source following the addition of 0.2% glucose (left) or fructose (right). **c,** Fold change of *BT1757* transcripts from *wild-type* (black) *or ΔBT1754* (red) 60 minutes following the addition of 0.2% fructose to cells cultured in media containing PMOG. **d,** Fructokinase activity of purified BT1757 protein. **e,** Growth of *wild-type* or *Δ BT1757* in minimal media containing fructose as the sole carbon source. **f,g,** Normalized bioluminescence from **(f)** *Δ BT1757* or **(g)** *ΔBT2493* harboring P-*fusA2* cultured in media containing PMOG (black) as sole carbon source or equal mixtures of PMOG and fructose (red) or glucose (blue). **h,** Fold change of *fusA2* (left) and *BT4295* (right) transcript amounts from *ΔBT2493* cultured in media containing PMOG as the sole carbon source following the addition of 0.2% glucose or fructose. For panels **a,e-g,** n=8; error is SEM in color matched shading. For panels **b,c,h,** n=6; error is SEM. *P*-values were calculated by 2-way ANOVA with Fisher's LSD test and * represents values < 0.05, ** < 0.01, *** < 0.001. For panel **d,** n=4; error is SEM.

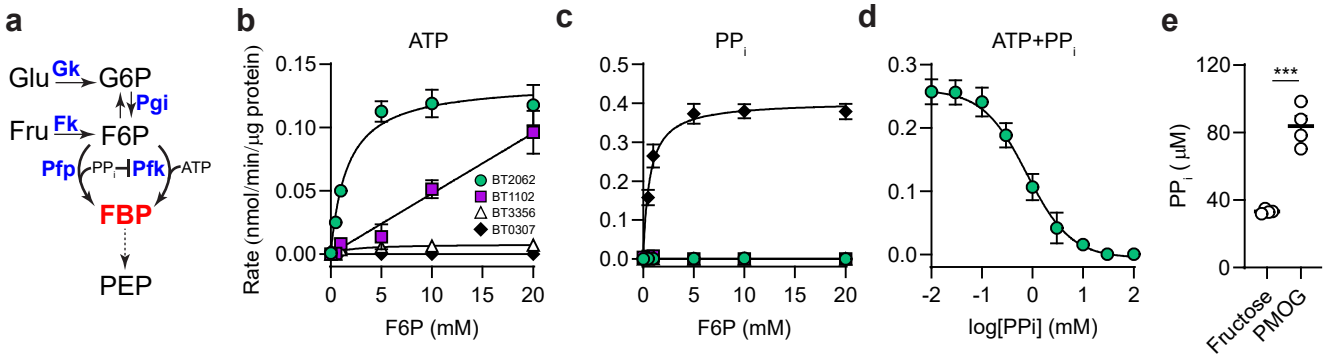

Fig. 3. Distinct enzyme classes synthesize FBP in *Bt*. a, Schematic of the EMP pathway in *Bt*. G6P=glucose-6-phosphate, F6P=fructose-6-phosphate, FBP=fructose-1,6-bisphosphate, PEP=phosphoenolpyruvate, Pgi=phosphoglucose isomerase, Pfp=phosphofructose phosphotransferase, Pfk=phosphofructokinase, PPi=pyrophosphate, ATP=adenosine triphosphate. **b,c,** Enzyme kinetics of purified BT2062 (circles), BT1102 (squares), BT3356 (triangles), or BT0307 (diamonds) in reactions containing either **(b)** ATP or **(c)** PPi as a phosphoryl donor. **d,** PfkA activity in the presence of increasing PPi amounts. **e,** PPi amounts in whole cell lysates of *wild-type Bt* grown in fructose or PMOG as the sole carbon source. For panels **b-d,** n=4, error is SEM. For panel **e,** n=4, error is SEM; *P*-values were calculated by 1-way ANOVA with Fisher's LSD test and *** represents values < 0.001.

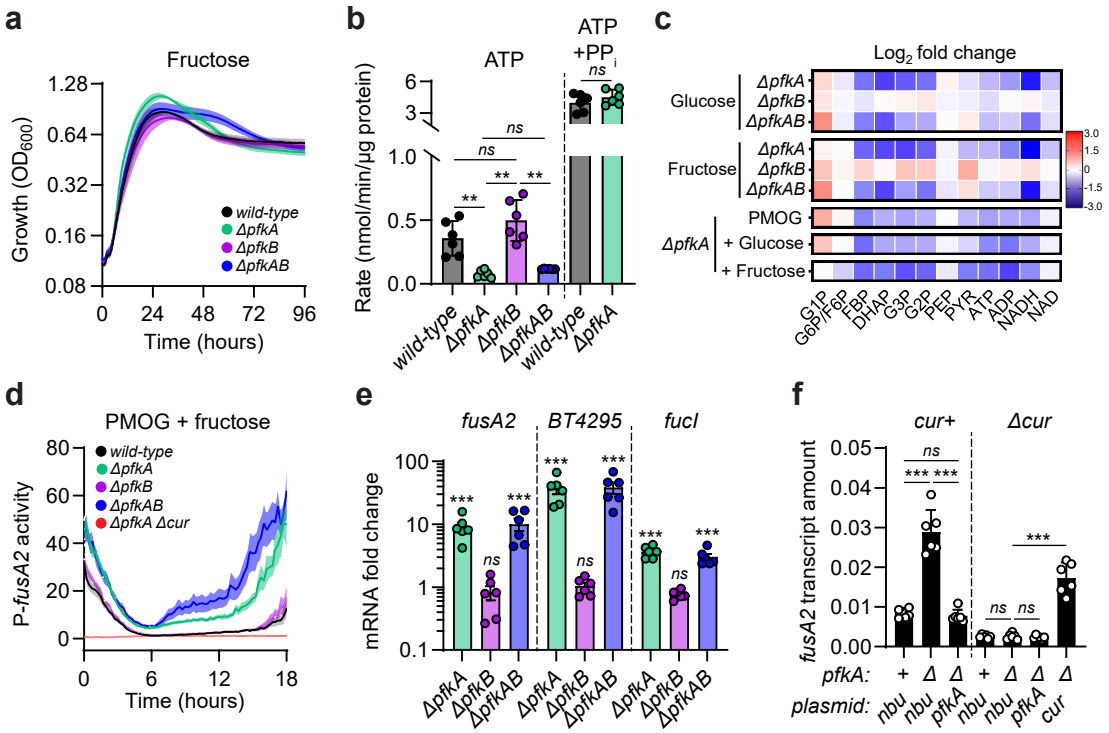

Fig. 4. ATP-dependent FBP production is required for Cur inhibition but dispensable for growth. a, Growth of *wild-type,* Δ*pfkA*, Δ*pfkB*, or Δ*pfkAB* in minimal media containing fructose as a sole carbon source. **b,** FBP synthesis measured from whole cell lysates of *wild-type,* Δ*pfkA*, Δ*pfkB*, or Δ*pfkAB*. **c,** Log_2 fold change of steady-state glycolytic intermediates in Δ*pfkA*, Δ*pfkB*, or Δ*pfkAB* in glucose, fructose, PMOG, PMOG with glucose, or PMOG with fructose. **d,** Bioluminescence from *wild-type* (black), Δ*pfkA* (green), Δ*pfkB (*purple), Δ*pfkAB* (blue*)*, or Δ*pfkA cur* harboring P-*fusA2* in minimal media containing equal amounts of PMOG and fructose. **e,** Fold change of *fusA2, BT4295, and fucI* transcript amounts relative to *wild-type Bt* from Δ*pfkA*, Δ*pfkB*, or Δ*pfkAB* cultured in minimal media containing fructose as a sole carbon source. **f,** *fusA2* transcript amounts in *wild-type*, Δ*pfkA*, Δ*cur*, Δ*pfkA* Δ*cur* harboring empty vector (*nbu*) or complementing plasmids grown in glucose as the sole carbon source. For panels **a,d,** n=8; error is SEM in color matched shading. For panels **b,e,f,** *P*-values were calculated by 2-way ANOVA with Fisher's LSD test and * represents values < 0.05, ** < 0.01, *** < 0.001. For panel **d,** n=4; error is SEM.

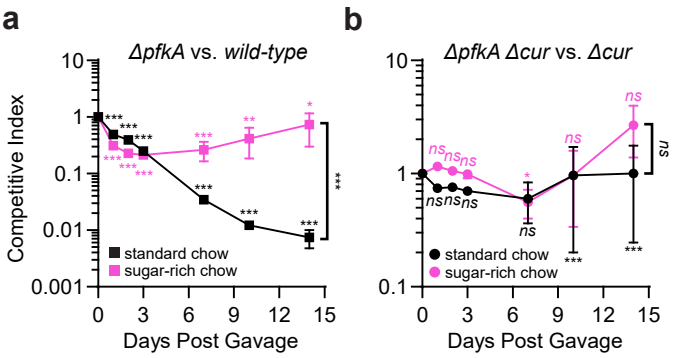

Fig. 5. ATP-dependent FBP production is required for intestinal fitness by controlling Cur. a, Competitive fitness of Δ*pfkA* co-introduced into germ-free mice with equal amounts of *wild-type Bt* and fed a standard polysaccharide rich chow (black, n=10) or a sugar-rich chow (pink, n = 8). **b,** Competitive fitness Δ*pfk* Δ*cur* co-introduced into germ-free mice with equal amounts of Δ*cur* and fed a standard polysaccharide rich chow (black, n=10) or a sugar-rich chow (pink, n=4). P-values were calculated using 2-way ANOVA with Bonferroni correction and * indicates values < 0.05, ** < .01, ***<.001.

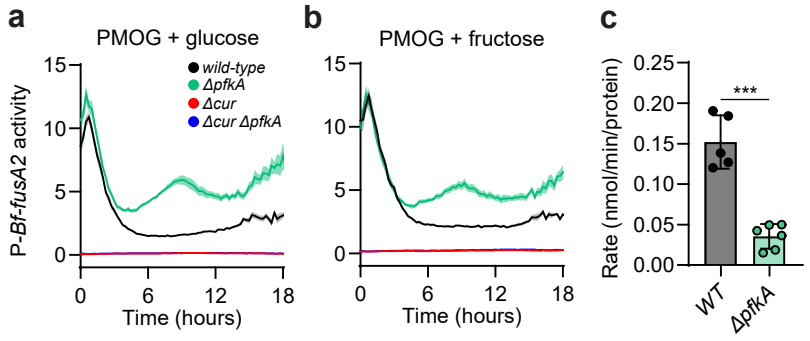

Fig. 6. *pfkA* is required for glucose- and fructose-mediated Cur inhibition and ATP-dependent FBP synthesis in *B. fragilis*. a-b, Bioluminescence from *wild-type Bf* (black), Δ*pfkA* (green), Δ*cur* (red), or Δ*pfkA* Δ*cur* (blue) harboring P-*Bf-fusA2* were cultured in media containing a mixture of equal amounts of PMOG and **(a)** glucose or **(b)** fructose. n=8 and error is SEM in color matched shading. **c,** FBP synthetic rates measured from whole cell lysates of *wild-type* or Δ*pfkA* supplied ATP or PPi as a phosphoryl donor. n=5 and error is SEM. P-values were calculated using an unpaired t-test and *** represents values < 0.001.

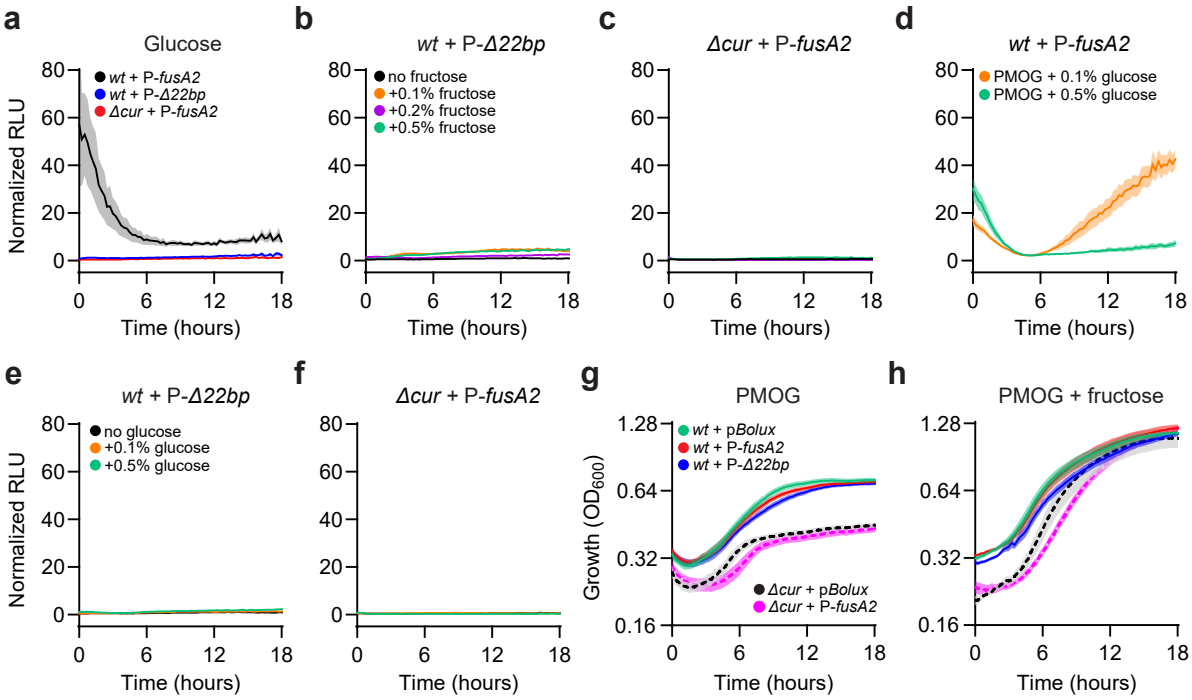

Extended Data Fig. 1. P-*fusA2* bioluminescence requires *cur*. a, Normalized bioluminescence from *wild-type* (black) or Δ*cur* (red) harboring P-*fusA2* or *wild-type Bt* harboring P-Δ*22bp* (blue) cultured in minimal media containing glucose as a sole carbon source. **b,c,** Normalized bioluminescence from **(b)** *wild-type Bt* harboring P-Δ*22bp* or **(c)** *cur* harboring P-*fusA2* cultured in PMOG alone (black) or in combination with 0.1% (orange), 0.2% (purple), or 0.5% (green) fructose. **d-f,** Normalized bioluminescence from *wild-type Bt* harboring **(d)** P-*fusA2* or **(e)** P-Δ*22bp*, or **(f)** Δ*cur* containing P-*fusA2* cultured in PMOG alone (black) or in combination with 0.1% (orange) or 0.5% (green) glucose. **g,h,** Growth of *wild-type Bt* (solid) or Δ*cur* (dashed) harboring p*Bolux* (black), P-*fusA2* (red), or P-Δ*22bp* (blue) grown in **(g)** PMOG alone or **(h)** equal amounts of PMOG and fructose. For all panels, n=8; error is SEM in color matched shading.

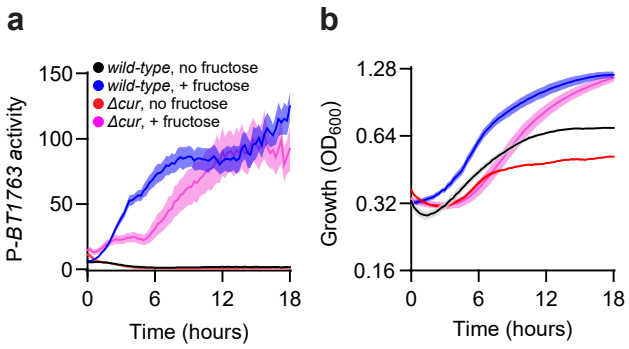

Extended Data Fig. 2. Cur is dispensable for fructose-inducible bioluminescence. a, Normalized bioluminescence from *wild-type Bt* or Δ*cur* harboring P-*BT1763* were cultured in PMOG alone (black & red, respectively) or in combination with 0.5% fructose (blue & pink, respectively). **b,** Growth of strains described in **(a)** in an equal mixture of 0.5% PMOG and fructose. For all panels, n=8; error is SEM in color matched shading.

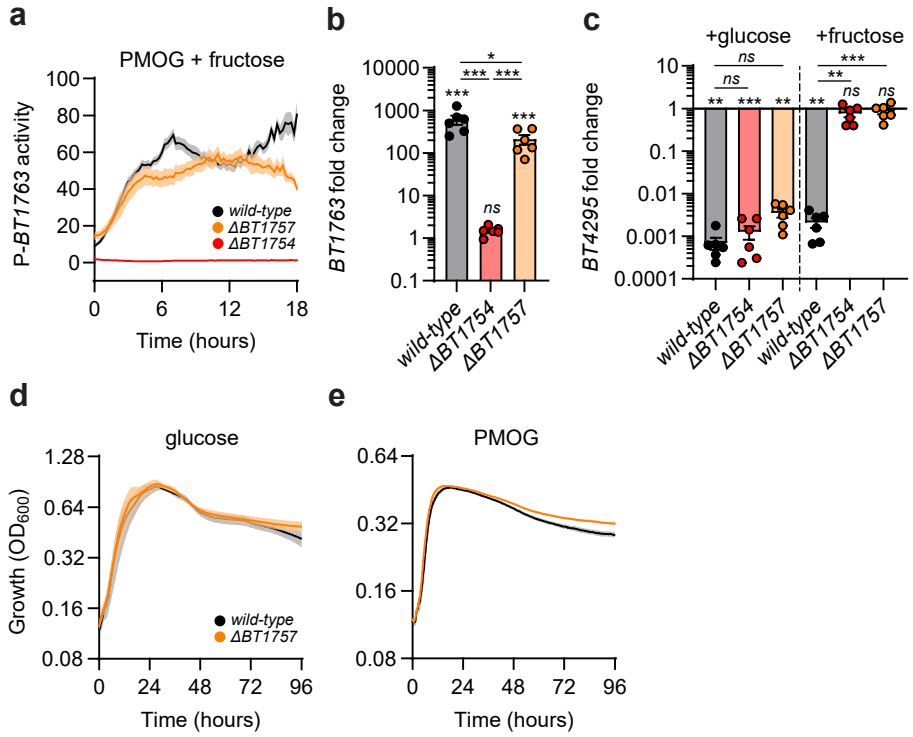

Extended Data Fig. 3. Fructose phosphorylation is dispensable for BT1754-dependent PUL activation but required for Cur inhibition. a, Normalized bioluminescence from *wild-type Bt* (black), Δ*BT1754* (red), or Δ*BT1757* (orange) harboring P-*BT1763* cultured in media containing equal amounts of PMOG and fructose. **b,** Fold change of *BT1763* transcript amounts from *wild-type Bt* (black), Δ*BT1754* (red), or Δ*BT1757* (orange) 60-minutes following the addition of 0.2% fructose to cells cultured in media containing PMOG as the sole carbon source. **c** Fold change of *BT4295* transcript amounts from *wild-type Bt* (black), Δ*BT1754* (red), or Δ*BT1757* (orange) following the addition of 0.2% glucose (left) or fructose (right). For panels **a,d,e,** n=8; error is SEM in color matched shading. For panel **b,** n=6; error is SEM; *P*-values were calculated by 1-way ANOVA with Fisher's LSD test. For panel **c,** n=6; error is SEM; *P*-values were calculated by 2-way ANOVA with Fisher's LSD test. For panels **c,d,** * represents values < 0.05, ** < 0.01, *** < 0.001.

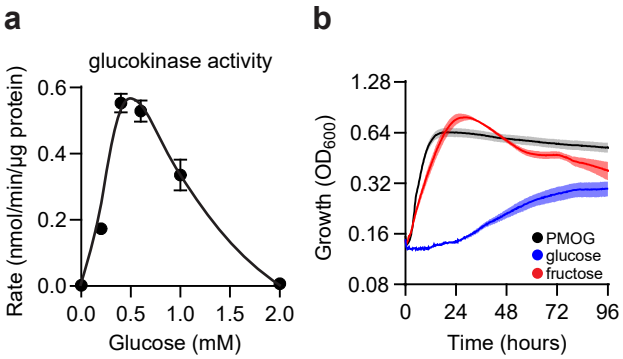

Extended Data Fig. 4. BT2493 faciliates glucose phosphorylation and utilization. a, Glucokinase activity of purified BT2493 protein. **b,** Growth of Δ*BT2493* in PMOGs (black), fructose (red), or glucose (blue) as sole carbon sources. For panel **a**, n=4; error is SEM. For panel **b**, n=8; error is SEM with color matched shading.

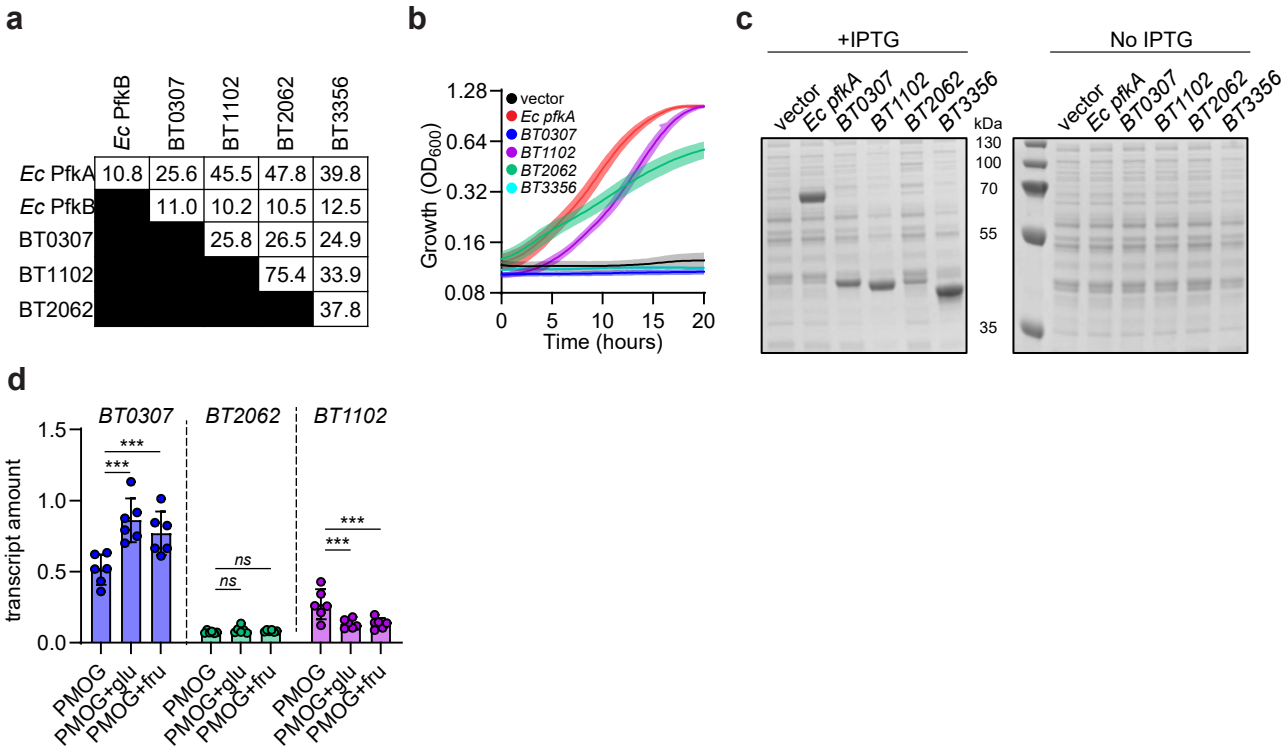

Extended Data Fig. 5. *Bt* possesses 2 bona fide Pfk enzymes. a, Amino acid sequence identity between *Ec* PfkA and PfkB with putative FBP biosynthetic enzymes in *Bt*. **b,** Growth of Δ*pfkAB Ec* harboring an empty vector (black), or a plasmid encoding *Ec pfkA* (red), *BT0307* (blue), *BT1102* (purple), *BT2062* (green) or *BT3356* (cyan) in minimal media containing glucose and 100 μM IPTG. **c,** Total protein from strains described in **(b)** grown in rich media with (left) or without (right) the addition of 100 μM IPTG. **d,** qPCR analysis of *BT0307*, *BT2062*, and *BT1102* transcript amounts from *wild-type Bt* grown in minimal media containing PMOG and 10- or 60- minutes following the addition of 0.2% glucose or fructose, respectively. For panel **b,** n=8; error is SEM with color matched shading. For panel **d,** n=6; error is SEM; *P*-values were calculated by 1-way ANOVA with Fisher's LSD test and * represents values < 0.05, ** < 0.01, *** < 0.001.

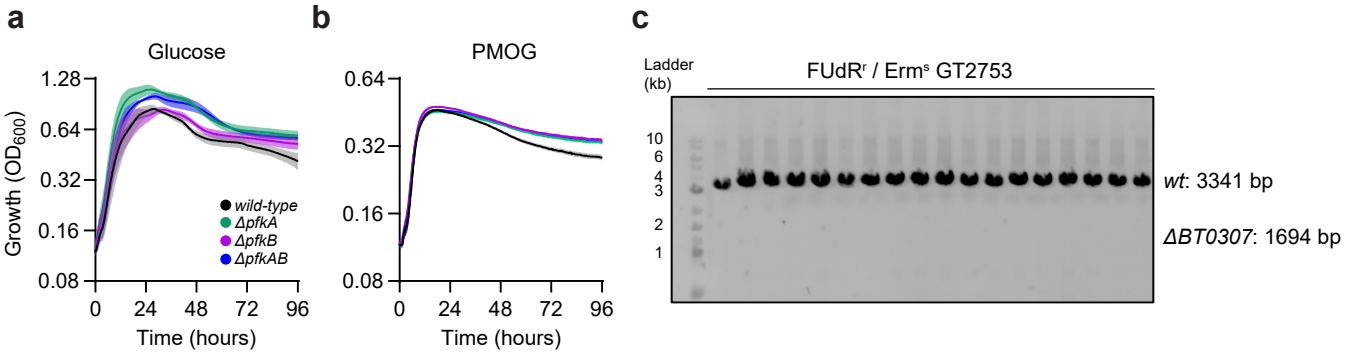

Extended Data Fig. 6. Phosphofructokinases are dispensiable for growth. a,b, Growth of *wild-type Bt*, *ΔpfkA*, *ΔpfkB*, or *ΔpfkAB* in minimal media containing **(a)** glucose or **(b)** PMOG as a sole carbon source. **c,** Putative *pfp* deletions examined by PCR analysis. For panels **a,b,** n=8; error is SEM with color matched shading.

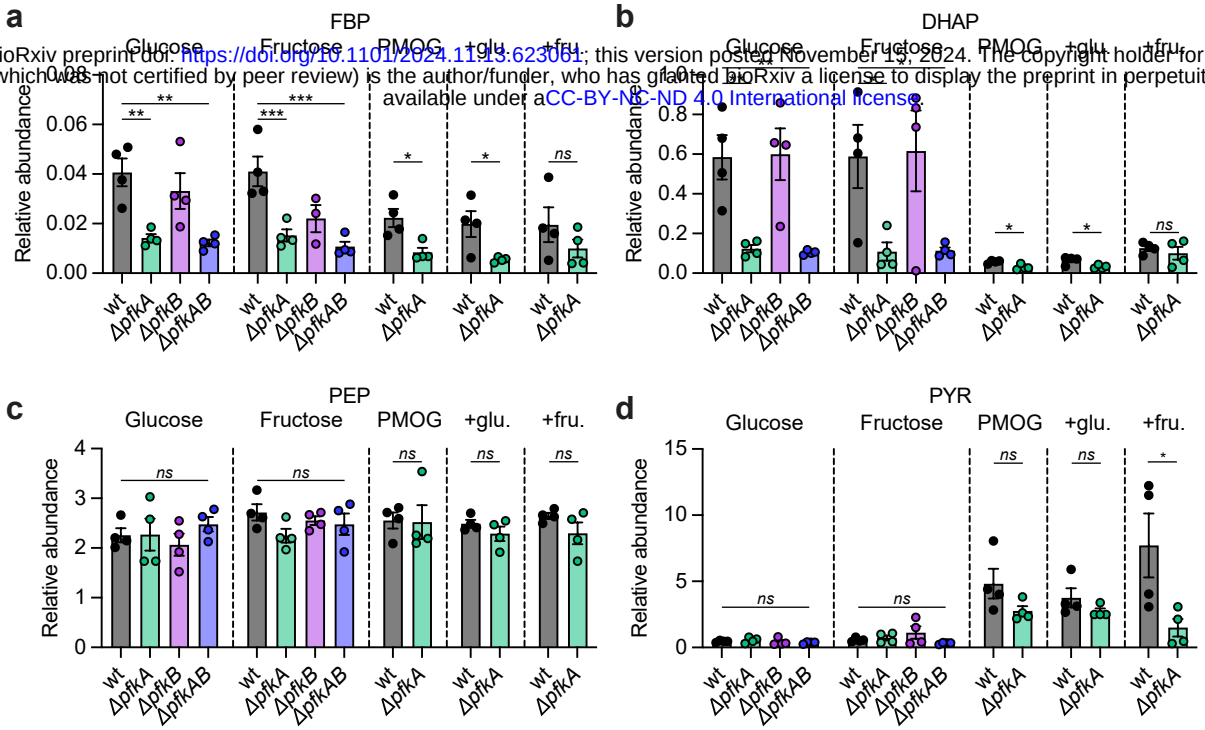

Extended Data Fig. 7. Relative abundance of glycolytic metabolites in *pfk* mutants. a-d, Relative amounts of FBP **(a)**, DHAP **(b)**, PEP **(c)**, or PYR **(d)** from *wild-type*, Δ*pfkA*, Δ*pfkB*, or Δ*pfkAB* grown in minimal media containing glucose, fructose, PMOG, PMOG with glucose, or PMOG with fructose as a sole carbon source. n=4; error is SEM. For glucose and fructose**,** *P*-values were calculated using 2-way ANOVA with Fisher's LSD test and * represents values < 0.05, ** < 0.01, *** < 0.001. For PMOG, PMOG with glucose, or PMOG with fructose, *P*-values were calculated using an unpaired t-test and * represents values < 0.05.

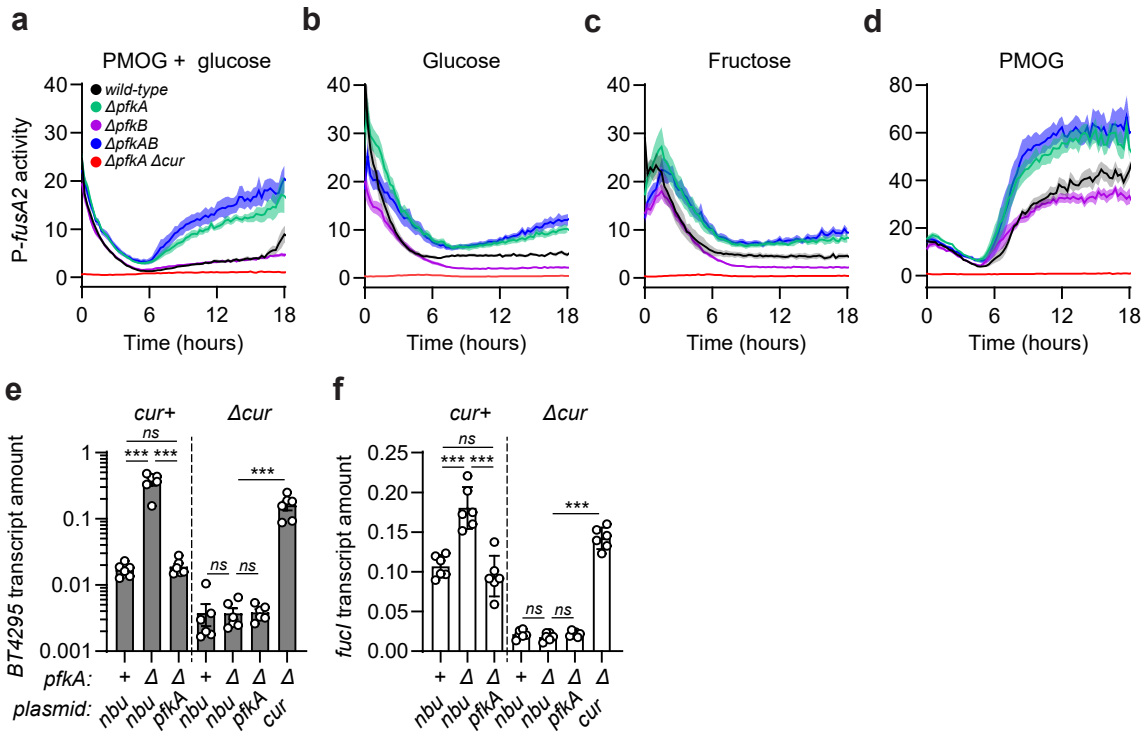

Extended Data Fig. 8. ATP-dependent FBP production silences Cur *in vitro*. a-d, Normalized bioluminescence from *wild-type Bt* (black), *ΔpfkA* (green), *ΔpfkB* (purple), *ΔpfkAB* (blue), or *ΔpfkA Δcur* (red) harboring P-*fusA2* grown in minimal media containing equal amounts of **(a)** PMOG and glucose, **(b)** glucose, **(c)** fructose, or **(d)** PMOG as a sole carbon source. **e,f,** *T*ranscript amounts of **(e)** *BT4295* or **(f)** *fucI* in *wild-type*, *ΔpfkA*, *Δcur*, or *ΔpfkA Δcur* harboring empty vector (*nbu*) or complementing plasmids grown in glucose as the sole carbon source. For panels **a-d,** n=8; error is SEM with color matched shading. For panels **e,f,** *P*-values were calculated by 2-way ANOVA with Fisher's LSD test and *** represents values < 0.001.

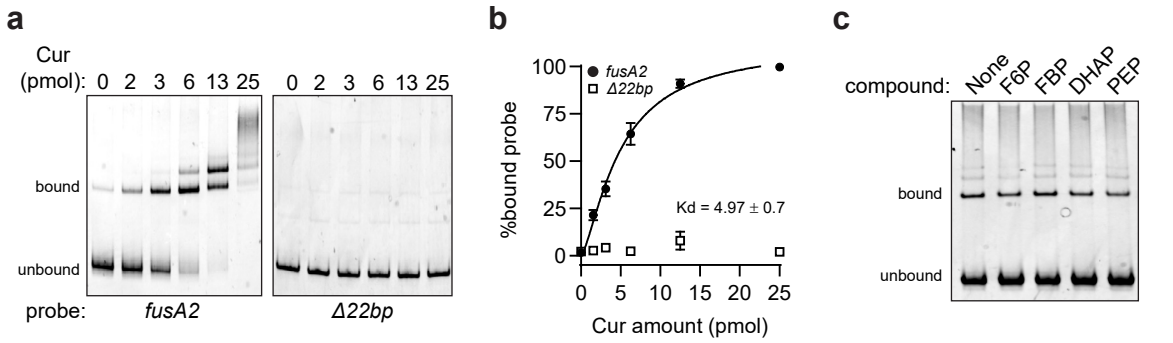

Extended Data Fig. 9. FBP does not alter *in vitro* Cur binding to the *fusA2* promoter. a, EMSA containing a *wild-type* or ∆*22bp fusA2* promoter DNA fragment co-incubated with the indicated amounts of Cur protein. **b,** DNA-binding saturation curve of **(a)**. **c,** EMSA assay containing 3 pmol of Cur protein was incubated with the *fusA2* promoter fragment and 1 mM of glycolytic intermediates. For panel **b,** n=3; error is SEM.

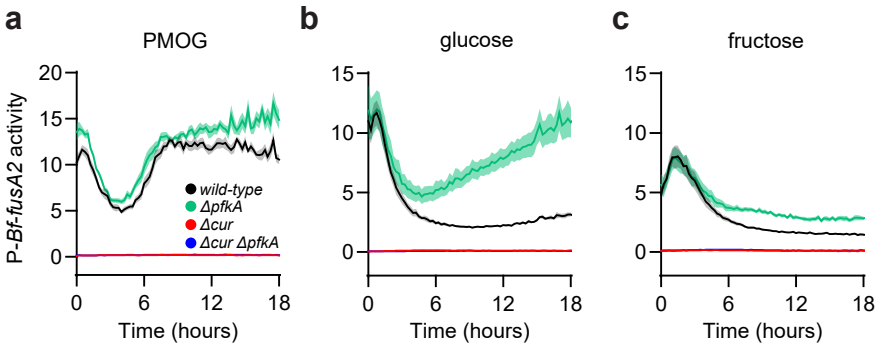

Extended Data Fig. 10. *pfkA* is required for Cur inhibition in *B. fragilis*. a-c, Normalized bioluminescence from *wild-type Bf* (black), Δ*pfkA* (green), Δ*cur* (red), or Δ*pfkA cur* (blue) harboring P-*Bf-fusA2* cultured in media containing **(a)** PMOG, **(b)** glucose, or **(c)** fructose as the sole carbon source. For all panels, n=8; error is SEM in color matched shading.